Astron. Astrophys. 358, 428–432 (2000)

ASTRONOMY AND ASTROPHYSICS

Parsec-scale jet behavior of NRAO 190 after a γ-ray outburst in August 1994

A. V. Yurchenko[1], **S. G. Marchenko-Jorstad**[1,2], **and A. P. Marscher**[2]

[1] Institute for Astronomy, St. Petersburg State University, Bibliotechnaya pl. 2, 198904 St. Petersburg, Russia
[2] Institute for Astrophysical Research, Boston University, 725 Commonwealth Ave., Boston, MA 02215, USA

Received 15 July 1998 / Accepted 31 January 2000

Abstract. We present the results of a three-year *Very Long Baseline Array* (VLBA) imaging campaign on the bright blazar NRAO 190 after it was identified as a source of a prominent γ-ray flare detected in August 1994 by the EGRET instrument on the *Compton Gamma Ray Observatory* (McGlynn et al. 1997). The source was observed at 22 GHz at 5 epochs and at 43 GHz once. As is typical for blazars, our results show a one-sided jet structure dominated by a bright, unresolved core with a prominent but gradually weakening knot moving down the jet with an apparent velocity of $8.5h^{-1}$c, ($H_o = 100h$ km s^{-1} Mpc^{-1}, $q_o = 0.5$). The time of ejection of this knot can be extrapolated, to within the errors, to the epoch of the aforementioned γ-ray flare. We interpret our results in terms of the "standard" relativistic shocked jet model (Blandford & Königl 1979; Marscher & Gear 1985). The angular resolution of the VLBA, together with the results of Metsähovi 22 GHz total flux monitoring, allow us to examine the brightness variations of separate source components. During the time of our monitoring, we observed the evolution of the source shortly after the peak of a major outburst and also during and after a lower amplitude flare. The first event created a strong, superluminally moving component, while the latter produced no significant changes in the jet structure. The characteristics of the jet were therefore different in the aftermath of each flare, possibly because the first disturbance generated rarefactions in its wake.

Key words: galaxies: active – galaxies: jets – galaxies: quasars: individual: NRAO 190 – radiation mechanisms: non-thermal – shock waves

1. Introduction

It has become common to interpret the observed nonthermal emission from blazars as coming mainly from synchrotron (radio to optical) and Compton (X- and γ-ray) processes in relativistic jets directed at small angles to the line of sight ($e.g.$, Blandford & Königl 1979). Under this scenario, apparent superluminal motions and flux variability in the radio band are explained by shock waves caused by fluctuations in the flow (Marscher & Gear 1985). Additional support for this concept comes from the observed fluxes and timescales of γ-ray variability of blazars, which demand that γ-ray emission must be strongly beamed, since in the isotropic case the density of radiation in the source would be so high that the photons would be lost to pair production (Mattox et al. 1993). Since both the radio and γ-ray properties of blazars require relativistic beaming, it is natural to assume that the radio and γ-ray emission originate in the jet and we can expect to see variations in the jet during or shortly after periods of strong γ-ray activity. Indeed, several cases with ejection of a new jet component near the time of observation of γ-ray flares or enhanced levels of γ-ray flux have been reported already (Otterbein et al. 1998 and references therein). Theoretically, there have been a number of promising numerical simulations of both the observed appearance and the spectrum of shocked relativistic jets ($e.g.$, Gómez et al. 1997; Bowman et al. 1996; Marscher & Travis 1996). The relativistic hydrodynamical simulations of Gómez et al. show complex structure behind the main shock of a disturbance in the jet flow, with both standing and secondary moving shocks and rarefactions that can be either transitory or long-lived. Each disturbance can therefore cause multiple apparent superluminal components as well as complex light curves. The most reliable way to explore whether such complexities actually exist is through direct, multi-epoch VLBI imaging of compact extragalactic jets.

NRAO 190 (IAU name 0440−003, $z = 0.844$; 1 mas = $4.16h^{-1}$ pc for $H_o = 100h$ km s^{-1} Mpc^{-1} and $q_o = 0.5$) is a typical flat-spectrum radio-loud QSO from which EGRET has detected significant γ-ray emission. It is highly variable at radio and optical wavelengths and shows fluctuations on all timescales, but it has not been detected as an X-ray source (upper limit of 0.088 μJy at 1 keV; Wilkes et. al 1994). VLBI maps at 8.4 and 2.3 GHz show a single compact component (Fey & Charlot 1997). The γ-ray flux detected from NRAO 190 in August 1994 by EGRET exceeded the "quiescent" state by at least an order of magnitude and corresponded to an isotropic luminosity of $8\text{x}10^{47}h^{-2}$ erg s^{-1} (McGlynn et al. 1997). Unless the beaming of γ-ray emission in the source is especially strong, the γ-ray luminosity is a major fraction of the total luminosity and may well dominate the expenditure of energy in the source during the flare. The flare (or series of flares) seemed to be rather

Send offprint requests to: S.G. Marchenko-Jorstad (jorstad@rjet.bu.edu)

Table 1. Parameters of the total flux and VLBA observations.

Epoch	Metsähovi		VLBA				
	Freq [GHz]	Flux [Jy]	Freq. [GHz]	Size of Beam [mas^2]	PA of Beam [deg.]	Map Peak [Jy/Beam]	Calib. Coeff.
1995.15	22	1.30	22	0.65x0.34	-0.2	0.61	1.00 ± 0.1
1995.47	37	1.17	43	0.44x0.15	-6.9	0.37	1.57 ± 0.2
1996.34	22	1.29	22	0.60x0.33	$+0.3$	0.58	1.18 ± 0.1
1996.60	22	0.95	22	0.65x0.35	-1.4	0.43	1.02 ± 0.1
1996.90	22	0.73	22	0.65x0.27	-2.7	0.34	1.39 ± 0.1
1997.58	22	1.10	22	0.63x0.36	-1.2	0.49	1.16 ± 0.1

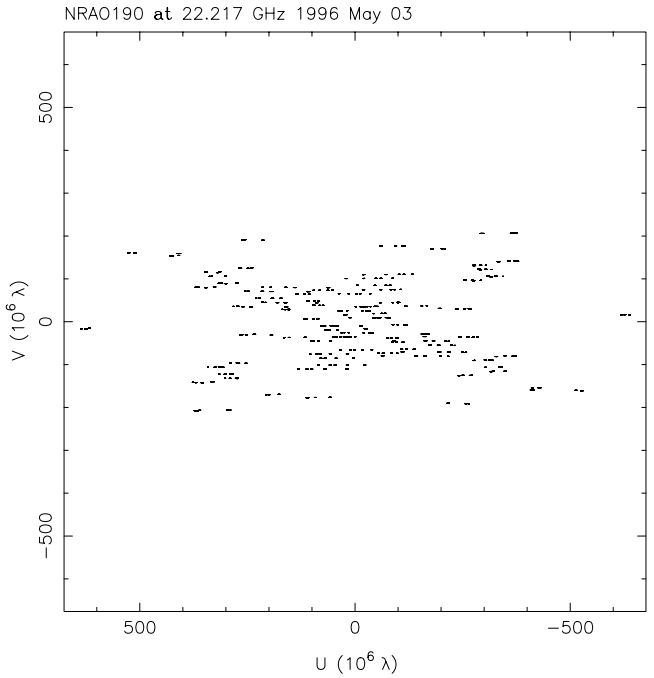

Fig. 1. The uv-coverage for the May 1996 VLBA observations.

prolonged, since EGRET detected a 3σ signal from the source 3 months prior to the major outburst.

At radio wavelengths the source was also in a high state shortly after the γ-ray flare, with a significant decline during the following months. however, both at optical and radio wavelengths the fluctuations detected were within historical limits (McGlynn et al. 1997).

2. Observations and data reduction

NRAO 190 was observed with the VLBA as part of a γ-ray bright blazar monitoring campaign at six epochs between 1995.1 and 1997.6 at frequencies (wavelengths) of 22 GHz (1.3 cm) and 43 GHz (7 mm; 1995 June 21). The observations were carried out with the VLBA recording system using four 8 MHz wide channels in both right and left circular polarization in "snapshot" mode with 3-4 scans of 5-15 minutes length each. Fig. 1 presents the typical uv-coverage.

The Astronomical Image Processing System (AIPS) software was used for post-processing and calibration. Corrections were made for zenith opacities, antenna gain curves, and system temperatures (the latter two supplied by NRAO). Imaging was performed using the CalTech software Difmap (Shepherd et al. 1994). We have performed both mapping with the CLEAN algorithm and model-fitting with elliptical gaussian components and find that there is very little visible difference between the two. The flux densities were adjusted a posteriori for discrepancies between the gain curves and actual antenna performance by requiring that the total fluxes on the images of nearly unresolved calibrating sources match the Metsähovi values. Table 1 lists the observed frequency and total flux measured at Metsähovi (interpolated to the epochs of VLBA observations), the observed VLBA frequency, the size and orientation of the interferometer beam (an elliptical gaussian approximation of the central portion),the peak brightness of the map, and calibration coefficients by which the nominal VLBA intensities are multiplied such that the total flux densities for the calibrating sources match the Metsähovi values.

Fig. 2 shows the hybrid maps obtained by convolving the delta-function clean components with an elliptical beam with dimensions corresponding to the average interferometer beam over all epochs at 22 GHz.

3. Results and Discussion

As can be seen on the VLBA images, the source is represented by a compact, one-sided jet with no evidence of extended structure beyond 2 mas from the core. On all of the 22 GHz maps the source displays three distinct components: a bright and unresolved core (A) at the eastern end of the jet, a bright knot (B) moving downstream from the core, and a weak component (C) that is apparently stationary with respect to the core. Therefore, we have adopted a three-component model to fit the uv-data. The results of model-fitting are summarized in Table 2. We used contours of constant χ^2 around the minimum to define confidence limits on the parameters. According to Pearson (1995) the 68.3% confidence range for a single parameter can be found by projecting the contour $\Delta\chi^2 = 1$ onto the axis corresponding to that parameter. We use the following procedure to determine errors for the fitted parameters: when best-fit model parameters have been found (i.e., χ^2 is minimized) one parameter (flux), two parameters (R and PA) or three parameters (a, b/a, and ϕ) are varied until χ^2 increases by 1 (other parameters are kept constant at their best-fit values). The difference between the val-

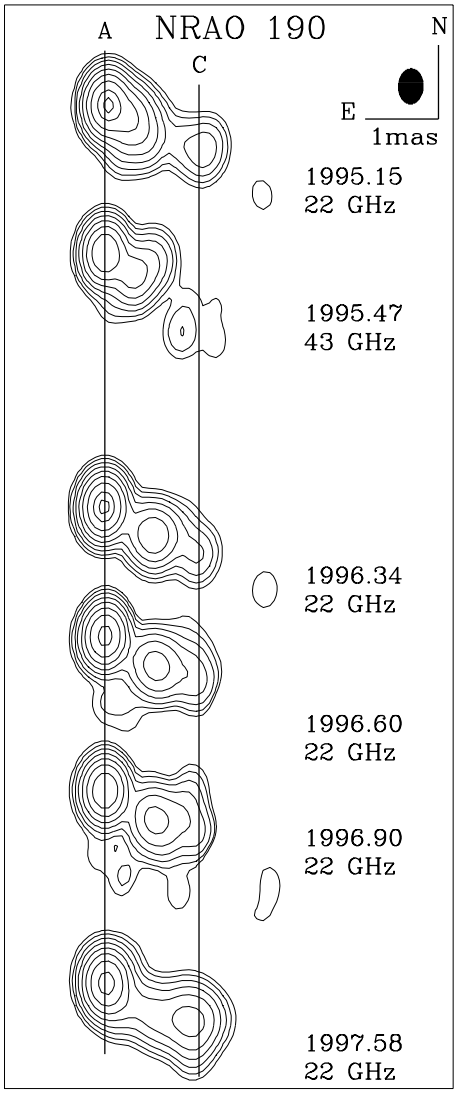

Fig. 2. Hybrid maps of NRAO 190. Contour levels are 0.5,1,2,4,8,16,32,64,90% of the peak brightness at epoch 1996.34 of 0.58 Jy/beam. The delta-function components are smoothed with an elliptical beam of 0.6×0.3 mas^2 at P.A. -1° (shown at the top right corner). The vertical lines A and C show the positions of the core and stationary component, respectively.

ues of the parameter corresponding to the two different values of χ^2 is taken as a measure of uncertainty, exept for the axial ratio b/a and the major axis position angle ϕ, which can not be estimated separately in Difmap. Meaningful errors could not be obtained for component C because it is weak and its position and flux are not well constrained by model-fitting. Nevertheless, we have indicated the estimated parameters of component C in Table 2 for completeness. These results show that component C is apparently stable in intensity and position over the time span of our data. We attribute the irregular shape of the low-level isophotes seen on the 1996.60 and 1996.90 map to the relatively high noise level and poor uv-coverage of the data, which resulted in strong side-lobes, rather than to more complex structure of the source.

Table 2. Summary of gaussian model fits.

Epoch	Comp.	Flux [Jy]	R [mas]	PA [°]	a [mas]	b/a	ϕ [°]
1995.15	A	0.43±0.09	0.0		0.16±0.03	0.42	-2
22 GHz	B	0.50±0.14	0.32±0.10	-137±18	0.26±0.02	0.68	21
	C	0.08	1.27	-123	0.48	0.64	-10
1995.47	A	0.33±0.07	0.0		0.18±0.05	0.28	-2
43 GHz	B1	0.25±0.10	0.50±0.09	-139±11	0.30±0.06	0.52	24
	B2	0.13±0.12	0.64±0.12	-110±13	0.24±0.08	0.18	-1
	C	0.03	1.24	-125	0.44	0.19	27
1996.34	A	0.73±0.06	0.0		0.06±0.03	0.21	-39
22 GHz	B	0.31±0.06	0.76±0.07	-129±5	0.27±0.02	0.79	-63
	C	0.07	1.31	-124	0.55	0.38	5
1996.60	A	0.45±0.05	0.0		0.14±0.02	0.44	-4
22 GHz	B	0.23±0.06	0.82±0.08	-132±6	0.36±0.04	0.58	-89
	C	0.06	1.33	-126	0.57	0.36	-7
1996.90	A	0.29±0.08	0.0		0.09±0.06	0.23	11
22 GHz	B	0.22±0.09	0.78±0.23	-125±17	0.30±0.06	0.37	-73
	C	0.06	1.23	-121	0.53	0.33	-3
1997.58	A	0.49±0.06	0.0		0.10±0.05	0.40	28
22 GHz	B	0.19±0.08	1.18±0.15	-120±7	0.44±0.08	0.91	30
	C	0.07	1.27	-121	0.55	0.38	5

Components B and C are completely blended at epoch 1997.58 and we cannot model them straightforwardly. But we note that, before this epoch, component C was quite constant (although weak) in brightness and position. Because of this and the similarity of the data quality and uv-coverage at epoch 1997.58 to those at epochs 1996.34 and 1996.60, we assume that the characteristics of component C remained the same. This allows us to estimate the position and flux of component B at epoch 1997.58.

The higher resolution and lower opacity of the 43 GHz data (Fig. 3) reveal a complex, irregular sub-structure for component B, with at least two gaussian components required to reproduce it (see components B1 and B2 at 1995.47 in Table 2). However, to enable comparison with the 22 GHz data, we treat it as a single feature: we obtain its total flux by adding fluxes from the two sub-components and estimate its radial separation from the core through a weighted average of the separation of the two sub-components.

Although, under the relativistic jet model, it is possible for gradients in the physical parameters to cause a frequency dependence in the apparent separation between the core and jet components, Otterbein et al. (1998) find this effect to be negligible in QSO 0836+710, and we will assume the same for NRAO 190. Hence, we plot data showing the separation of component B from the core as a function of time for both frequencies in the same graph (Fig. 4). It is seen that a straight line passes through all the data with the largest deviations corresponding to the 1995.47 data at 43 GHz and 1996.90 data at 22 GHz, for which the uv-coverage is worst. It therefore appears that the proper motion of component B is constant to within the uncertainties. Table 2 shows that the position angle of component B is also constant, except possibly for the last epoch (1997.58).

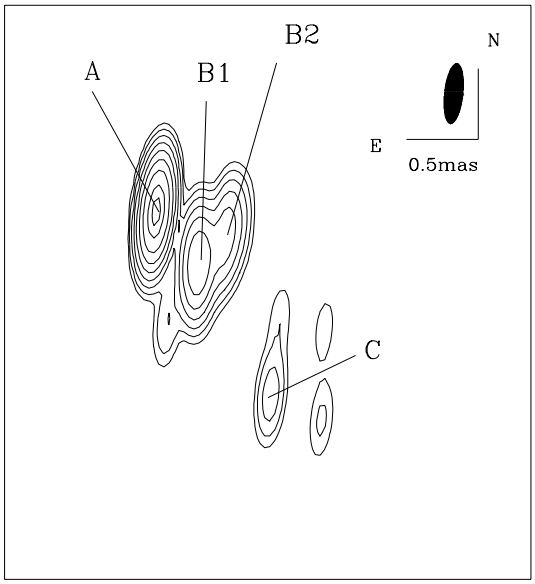

Fig. 3. Hybrid map of NRAO 190 at 43 GHz at epoch 1995.47. Contours are 0.5,1,2,4,8,16,32,64,90% of the peak brightness, which is 0.367 Jy/beam. The corresponding beam (0.45×0.15 mas^2 at P.A. -7°) is shown at the top right corner.

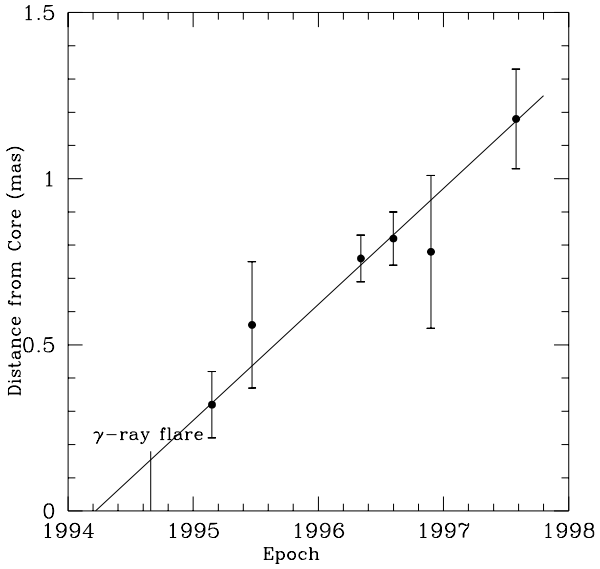

Fig. 4. Relative separation between the core and the ejected component B.

The solid line represents a least squares fit corresponding to 0.34 ± 0.03 mas yr^{-1}, which translates into $8.5\pm0.8h^{-1}$c. The linear extrapolation yields a date of zero separation 160 ± 70 days before the observed γ-ray flare in August 1994; however, it is unknown when this outburst started: three months prior, EGRET also detected NRAO 190 at the 3.3σ level. Hence, there may have been a prolonged high γ-ray state that started near the time of the ejection of component B.

The light curves corresponding to the 22 GHz flux of the core and component B are shown in Fig. 5. The values indicated for epoch 1995.47 are estimated from the 43 GHz measurements.

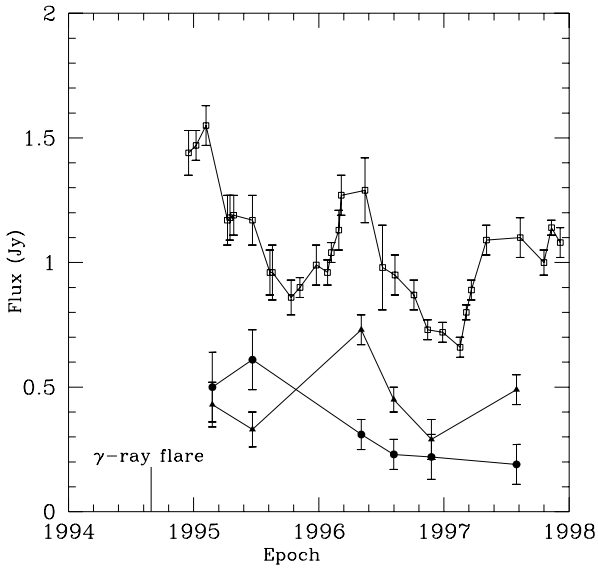

Fig. 5. Brightness variations of separate components. Open squares denote the total 22 GHz flux measured at Metsähovi, triangles and circles denote the flux from components A and B, respectively.

These values assume that component B is optically thin with a power-law spectral slope of -0.7 ($S\propto\nu^{\alpha}$), which is commonly used (e.g., Otterbein et al. 1998) to represent a synchrotron jet component, and that the core has a flat spectrum. While the jet component B progressively weakens, the flux of the core region fluctuates by a factor of ~ 2, matching approximately the total flux variations (also plotted in Fig. 5). This variation may be caused either by the variability in the core itself or by the production of a new moving component. One could expect the latter on the basis of the similarity between the 22 GHz light curves of the events in 1995 and 1996, in which there is an inflection during the decay phase starting $\sim$0.2 yr after each maximum. In the 1995 flare this inflection coincides with an increase in the flux of component B (although the estimate of the component flux at 22 GHz at this epoch has been obtained from the component flux at 43 GHz and a value of the spectral index -0.7). However, no new component appears on our maps during or after the 1996.34 flare, despite the high quality of the VLBA data in 1996.34 and 1996.60. Nevertheless, it is possible that a new component was "born" during the 1996 flare because the gaussian model fitting gives a core size more than twice as large at epoch 1996.60 as at epoch 1996.34 (see Table 2), when the peak of the core brightness was observed. After emerging from the core region, this new component may have become weak by encountering a rarefaction in the wake of the major disturbance that created component B (see Gómez et al. 1997). It is also possible that no new component appeared after the 1996 flare, indicating that the behaviour of the source is not identical for all radio flares.

4. Conclusions

The near coincidence of the peak in the γ-ray light curve and epoch of ejection of superluminal component B suggests

that the quasar NRAO 190 is another example of a blazar which shows a connection between γ-ray variability and high-resolution VLBI structure. These results can be explained by the relativistic shocked jet model (superluminal motion, exponential flux decay), which associates strong γ-ray emission and the appearence of a new component with a shock wave. The different structure in the jet following the two main radio flares observed in NRAO 190 in 1995 and 1996 demonstrates that the properties of the jet change from one event to the next. Further high-frequency VLBI monitoring of core-jet sources can determine whether such changes are consistent with those seen in hydrodynamical simulations.

Acknowledgements. We are grateful to H. Teräsranta for providing 22 and 37 GHz flux density measurements from the Metsähovi Radio Station in Finland. Part of this work was supported by the Russian Federal program "Integration", grant #578, a grant from the State Committee of Higher Education and grant # 98-02-16609 from Russian Fund of Basic Research. The VLBA observations presented in this paper were funded in part by NASA through CGRO Guest Investigator Program grants NAG5-2508, NAG5-3829 and NAG5-7323.

References

Blandford R.D., Königl A., 1979, ApJ, 232, 34
Bowman M., Leahy J.P., Komissarov S.S., 1996, MNRAS, 279, 899
Fey A.L., Charlot P., 1997, ApJS, 111, 95
Gómez J.L., Martí J.M., Marscher A.P., Ibáñez J.M., Alberdi A., 1997, ApJ, 482, L33
Marscher A.P., Gear W.K., 1985, ApJ, 298, 114
Marscher A.P., Travis J.P., 1996, A&AS, 120, C537
Mattox J.R., Bertsch D.L., Chiang J., et al., 1993, ApJ, 410, 609
McGlynn T.A., Hartman R.C., Bloom S.D., et al., 1997, ApJ 481, 625
Otterbein K., Krichbaum T.P., Kraus A., Lobanov A.P., Witzel A., Wagner S.J., Zensus J.A., 1998, A&A, 334, 489
Pearson T.J., 1995, In: Zensus J.A., Diamond P.J., Napier P.J.(eds.), PASPC, 82, 281
Shepherd M.C., Pearson T.J., Taylor G.B., 1994, BAAS 26, 987
Wilkes B.J., Tanenbaum H., Worrall D.M., Avni Y., Oey M.S., Flanagen J., 1994, ApJS, 92, 53
Zensus J.A., 1997, ARAA, 35, 607